Environmental Engineering and Management Journal

January 2020, Vol. 19, No. 1, 1-9
http://www.eemj.icpm.tuiasi.ro/; http://www.eemj.eu

"Gheorghe Asachi" Technical University of Iasi, Romania

STUDY OF BATCH ADSORPTION OF URANIUM IONS BY MCM-48 MATERIALS SYNTHESIZED AT ROOM TEMPERATURE

Meriem Chabane Sari[1,2], Abdelkader Namane[2]*, Jazia Arrar[2], Redouane Mélikchi[1], Rabah Kerbachi[2]

[1]Department of Material Process Engineering of the Nuclear Research Center of Draria, BP 43 Sebala, Draria, Algiers, Algeria
[2]Laboratory of Environmental Science and Technology of the National Polytechnic School, 10 Hassen Badi Avenue, BP 12, 16200 El Harrach, Algiers, Algeria

Abstract

The mesoporous MCM-48 was synthesized at room temperature with different templates such as hexadecytrimethylammonium bromide (C_{16}TABr), hexadecytrimethylammonium chloride (C_{16}TACl) and dodecyltrimethlammonium chloride (C_{12}TACl). The obtained materials were characterized by XRD, N_2 adsorption/desorption, FTIR and SEM techniques, and their performance as uranium adsorbent were investigated. In this framework, the effect of contact time, pH of solution, initial uranium concentration and temperature were investigated in batch reactor.
The results showed that the adsorption process was favorably fitted with the second-order kinetic model and the isotherm obeys to Langmuir model. Moreover, the maximum adsorption capacity of MCM-48 for uranium (VI) was of the order of 160 mg/g. The thermodynamic parameters indicated that the sorption of uranium ions on MCM-48 materials was a spontaneous and endothermic process.

Keywords: adsorption, characterization, MCM-48, synthesis, uranium

Received: January, 2019; Revised final: April, 2019; Accepted: June, 2019; Published in final edited form: January, 2020

1. Introduction

In the last decade, the problem of metals has become an important subject, especially in contaminated waters. Because they are toxic and non-biodegradable, and both their accumulation and transfer pose not only a huge risk to the environment, but also to human health, even trace levels. Uranium is a toxic radioactive element arising from nuclear industry (mining, production of nuclear fuels, laboratory etc.). It is usually found in the environment in the form hexavalent (VI^+), the mobile, aqueous uranyl ion UO_2^{2+} (Krestou et al., 2003). Its concentration in drinking water, which is recommended by the United States Environmental Protection Agency (USEPA) is 0.03 mg/L. The permissible discharge levels for nuclear industries range from 0.1 to 0.5 mg/L (Anirudhan et al., 2010). Several methods were used for the removal of uranium ions from aqueous solutions, such as chemical precipitation (Krestou et al., 2004), solvent extraction (Shen et al., 2011), membrane filtration (Chellam and Clifford, 2002), flotation (Prasada Rao et al., 2006) and ion exchangers (Lee et al., 2002). Among these methods, adsorption is the most attractive and effective way to remove uranium from aqueous solution, due to its highly removal efficiency, low cost and simplicity of implementation (Reza et al., 2018; Zhang et al., 2015). Several works have explored the adsorption ability of a several materials such as resin, zeolitic materials, carbon, carbon nanotube composites, biomass, mesoporous materials, for removing uranium ions from aqueous solutions (Chen et al., 2018; Dan et al., 2016; Elabd et al., 2014; Mellah et al., 2006). Nevertheless, poor selectivity, low surface area and capacity restricted their use (Selvam et al., 2001).

Since 1992, a new family of ordered mesoporous silica named M41S was synthesized by Kresge et al.

* Author to whom all correspondence should be addressed: e-mail: abdelkader.namane@g.enp.edu.dz; Phone: 00213699281573

(1992) and Beck et al. (1992). These solids are prepared by hydrothermal transformation of basic silicate or aluminosilicate gels in the presence of quaternary ammonium surfactants, $C_nH_{2n+1}(CH)_3\ N^+X^-$, with different alkyl chain lengths and counter ion (n=12, 14, 16, 18; X=Br, Cl and OH). The M41S family includes hexagonal MCM-41, cubic MCM-48, and unstable lamellar MCM-50 mesostructures (Matei et al., 2016). The characteristic properties of these materials are of a high surface area and an ordered pore distribution, with homogenous sizes in the range of 2-10 nm. Their pore size can be tailored through the proper choice of surfactant used as template, auxiliary chemicals and reaction conditions (Koyano and Tatsumi., 1997).

The MCM-48 is the most attractive material from M41S family, owing to its three-dimensional, interconnected channels, providing more advantages including fast diffusion and resistance to pore blocking of coming molecules over the one-dimensional pores of MCM-41 (Maneesuwan et al., 2013). Moreover, due to its long-range order, large surface area, and narrow pore size distribution, MCM-48 has been used as an adsorbent, catalyst, and catalyst support.

Generally, to obtain MCM-48, the most widely used raw materials are hexadecytrimethylammonium bromide (CTAB) as a surfactant, sodium hydroxide (NaOH) as a catalyst, and tetraethylorthosilicate (TEOS) as a silica source, using conventional autoclave heating for several days (Longloiler et al., 2011; Wang et al., 2009).

The aim of this study is to synthesize MCM-48 materials under accessible operating conditions (room temperature and short reaction time), using three directing agents, namely hexadecytrimethylammonium bromide (C_{16}TABr), cetyltrimethylammonium chloride (C_{16}TACl) and dodecyltrimethlammonium chloride (C_{12}TACl), NH_4OH as catalyst and TEOS as silica source.

In an intent to use it as adsorbents to remove uranium from contaminated waters, the effects of various operational conditions, such as contact time, solution pH, initial uranium concentration and temperature were determined.

2. Experimental

2.1. Chemicals used

C_{16}TABr (96%, Fluka), C_{16}TACl (25% in H_2O, Aldrich), C_{12}TACl (98%, Fluka) were used as the structure directing agent and TEOS (98%, Aldrich) as source of silica. Ethanol absolute C_2H_5OH (analytical grade, Merck), ammonia solution NH_4OH (29%, Prolabo) and deionized water were used as reagents for the synthesis.

Uranyl nitrate hexahydrate $UO_2(NO_3).6H_2O$ (99%, Merck) was used for the preparation of uranium stock solution at 1 g/L. The working solutions were prepared by proper dilution from the stock solution. The pH of each solution at the start experiment was adjusted to the required value with diluted nitric acid (HNO_3) and sodium hydroxide (NaOH) solutions.

2.2. Synthesis of mesoporous silica

The MCM-48 materials were prepared individually using three structure directing agents: (a) C_{16}TABr, (b) C_{16}TACl, (c) C_{12}TACl. In a typical synthesis 2.65 g, 9.09 g and 1.92 g of each template C_{16}TABr, C_{16}TACl, C_{12}TACl, respectively were added to 120 ml of deionized H_2O and 50 mL of ethanol under stirring. After complete dissolution, 12 mL of NH_4OH were added, and after 5 min 3.6 mL of TEOS. The sample is stirred vigorously during 16 hours at room temperature. The obtained solid was recovered by filtration, washed with deionized water and dried overnight at room temperature. The templates were removed by calcination at 540°C for 6 hours.

2.3. Adsorption batch experiment

The batch uranium adsorption experiments were carried using out in polypropylene flasks containing 21 mg of the different MCM-48 adsorbents (a; b; c) suspended in 15 mL of uranium solution at the selected pH. The flasks were agitated on a shaking table at 160 rpm for different contact times, initial pH of uranium solution, uranium concentration and temperatures. The solution was separated from the adsorbents by centrifugation. Then the initial and residual uranium concentrations were measured on a UV-spectrophotometer (JASCO V-530) using Arsenazo III method at a wavelength of 652 nm.

The amount of the adsorbed uranium q (mg/g) on the different MCM-48 and distribution constant (K_d) (L/g) were calculated using the following equations (Eqs. 1-2):

$$q = (C_i - C_{eq}).\frac{V}{m} \tag{1}$$

$$K_d = \frac{(C_i - C_{eq})}{C_{eq}}.\frac{V}{m} \tag{2}$$

where C_i (mg/L) is the initial uranium concentration, C_e (mg/L) is the residual uranium concentration at equilibrium; V (L) is the volume of uranium solution; m (g) is the weight of the different MCM-48 tested as adsorbents.

2.4. Characterization of the material

X-ray powder diffraction data of the elaborated materials were collected on a diffractometer (XPERT) using CuKα radiation in the 2θ range of 1.7-10° with a scan speed of 0.02°/min. N_2 adsorption–desorption isotherms were recorded using "Micomeritics ASAP2010" at 77 K. Prior to this analysis, calcined samples were degassed at 250°C for 22h. The surface area was determined by using BET method. The pore volume, and pore diameter were calculated by using the BJH model.

FTIR-spectra were obtained on a PerkinElmer apparatus, "model Spectrum two L1600301", in 4000-

400 cm^{-1} region, using UATR technique. To determine the sample particle size and morphology, the scanning electron micrographs (SEM) of different samples were performed on a "Joel 6360LV" intensively operated.

The pH of point of zero charge *(pH_{PZC})* of different MCM-48 was determined using the method described by (Cerovic et al., 2007). 20 mL aliquots of a solution of KNO_3 (0.01M) are adjusted to pH between 2-12 using NaOH (0.1N) and HNO_3 (0.1N) solutions. 0.1 g of different the adsorbents were placed in the different solutions and stirred for 24 hours. The final pHs of the different filtered solutions are measured; the pH_{PZC} corresponds to the value where the final pH and the initial pH have equal values.

3. Results and discussion

3.1. Characterization

3.1.1. X-ray diffraction

Fig. 1 shows the XRD patterns of the synthesized MCM-48 using C_{16}TABr, C_{16}TACl and C_{12}TACl as templates.

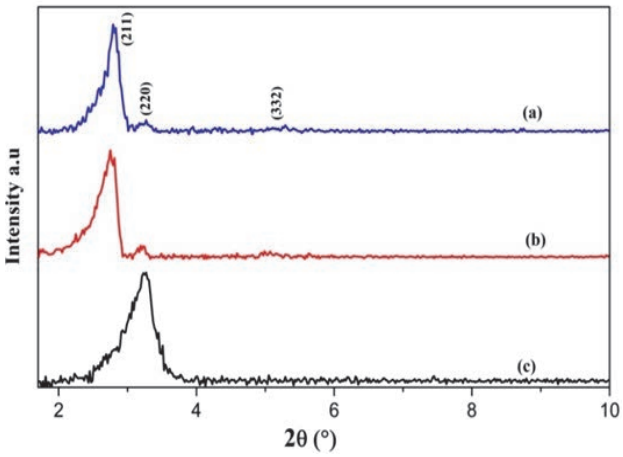

Fig. 1. XRD patterns of MCM-48 materials with different templates: (a) C_{16}TABr, (b) C_{16}TACl, (c) C_{12}TACl

The observed diffraction peaks at 2.7°, 3.2° and 5.2° corresponds respectively to (211), (220) and (332) plans according to the ASTM card N° 00-050-0511. These peaks are characteristics of Ia3d cubic structure of MCM-48 mesoporous materials (Schmidt et al., 1995). Approximately, similar diffraction patterns are observed in the case of MCM-48 prepared using C_{16}TABr and C_{16}TACl templates where (211) is the main peak in agreements with results (Melendez-Ortiz et al., 2014). However, in the case of MCM-48 prepared using C_{12}TACl template, the main peak is (220). This structure modification is probably responsible of the MCM-48 properties improvement (see results below). Duduman et al. (2018) found that the crystallinity degree increased by calcination.

3.1.2. Surface characterization

BET analysis technique encompasses external area and pore area evaluations to determine the total specific surface area yielding important information in understanding the adsorption mechanism. On the other hand, the Barrett–Joyner–Halenda (BJH) analysis allows determining pore area and specific pore volume using adsorption and desorption techniques. Both techniques are complete for the characterization of an adsorbent.

Nitrogen adsorption/desorption isotherms of elaborated materials with different templates are shown in Fig. 2. According to the IUPAC nomenclature, these isotherms can be classified as type IV, typical of mesoporous materials (Brunauer et al., 1940). Moreover, the observation of an abrupt rise at 0.2 relative pressure for the MCM-48 formed with C_{16}TABr and C_{16}TACl as template (Figs. 2 (a), (b)) due to capillary condensation is representative of mesoporous materials (Miriam et al., 2006).

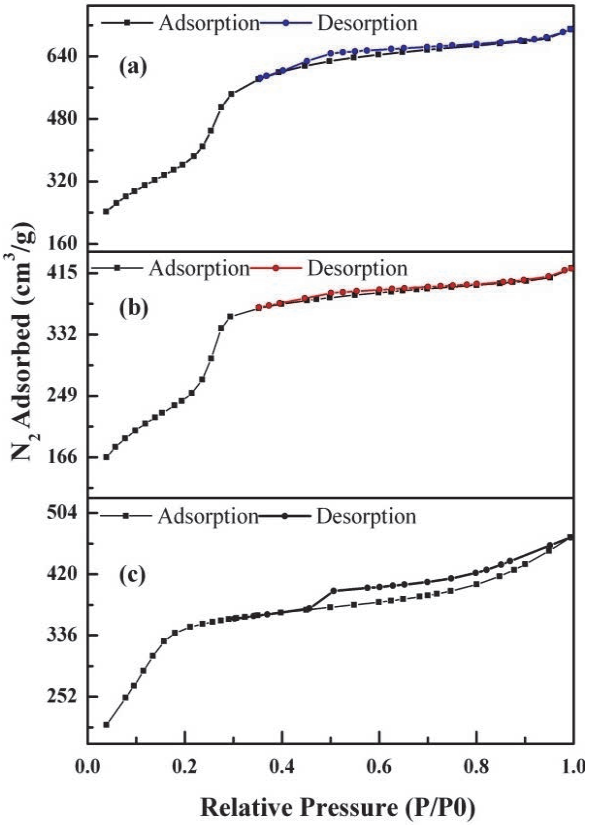

Fig. 2. Nitrogen adsorption desorption isotherms of MCM-48 materials with different templates:
(a) C_{16}TABr, (b) C_{16}TACl, (c) C_{12}TACl

All isotherms present H4 type hysteresis, assigned to slit shaped pores (Kumar et al., 2003). The isotherms are also characterized by a small hysteresis loop in the range of p/p_0 of 0.4-0.8, which is ascribed to the inter-particle volume. Table 1 presents the textural characteristics for the MCM-48 materials.

Table 1. Textural characteristics for the MCM-48

Samples	*S_{BET} (m^2/g)*	*Pore volume (cm^3/g)*	*Pore diameter (nm)*
MCM-48(a)	1334	1.05	2.57-4.58
MCM-48(b)	900	0.38	2.33-5.99
MCM-48(c)	1418	0.54	2.77-5.91

Table 2. Comparison of the physical characteristics of MCM-48 (a) with similar materials

Materials		*MCM-48 Chen et al. (2013)*	*MCM-48 Longloilert et al. (2011)*	*MCM48 (a) Present work*
Synthesis conditions	Temperature(°C)	110	140	25
	Time (h)	72	16	16
Characteristics	S_{BET} (m^2/g)	961	1288	1334
	Pore diameter (nm)	4.16	2.86	2.57-4.58
	Pore volume (cm^3/g)	1.00	0.92	1.05

This table shows high specific surface area values which are obtained for all MCM-48 materials (higer than 900m^2/g). Their pore diameters are calculated by the BJH model that vary from 2.3 nm to 6.0 nm. Consequently, MCM-48 materials possess intrinsic characteristics that can lead to interesting adsorptive capacities.

The comparison of MCM-48 (a) with similar synthesized materials is summarized in Table 2. It is found that the characteristics are comparable, although the synthesis conditions are different.

3.1.3. FTIR results

As shown in Fig. 3, similar FTIR spectrums were obtained for the different materials. The adsorption broad band in 3000-3700 cm^{-1} regium, with maximum at around 3376 cm^{-1}, is due to the O-H stretch of silanol group's (Tavakoli et al., 2013).

The band in region 1050-1080 cm^{-1} was attributed to the asymmetric stretching of Si-O-Si groups. The peak at around 960 cm^{-1} was assigned to the Si-O stretching vibration of Si-OH groups. The symmetric stretching of Si-O-Si groups was observed at ~ 800 cm^{-1} and the peak at 460 cm^{-1} is due to the bending mode of Si-O-Si, which are the characteristic adsorption peaks of SiO_2. This indicates that the structure of the materials has not been damaged during the calcination step (Zuo et al., 2011).

3.1.4. SEM analysis

Fig. 4 shows that the different templates used did not induce any notable morphological changes. All samples showed a spherical morphology with sizes from 200 to 600 nm for C_{16}TABr 100 to 500 nm for C_{16}TACl and 200 to 700 nm for C_{12}TACl.

3.2. Sorption studies

3.2.1. Effect of contact time

The effect of contact time on the adsorption of U(VI) ions onto different MCM-48 was investigated for contact time varying from 0 to 10 hours. The experiments were performed at room temperature with an initial concentration of U(VI) of 50 mg/L. The experimental results are presented in Fig. 5. The uptake was found to be fast and increases with an increase in contact time.

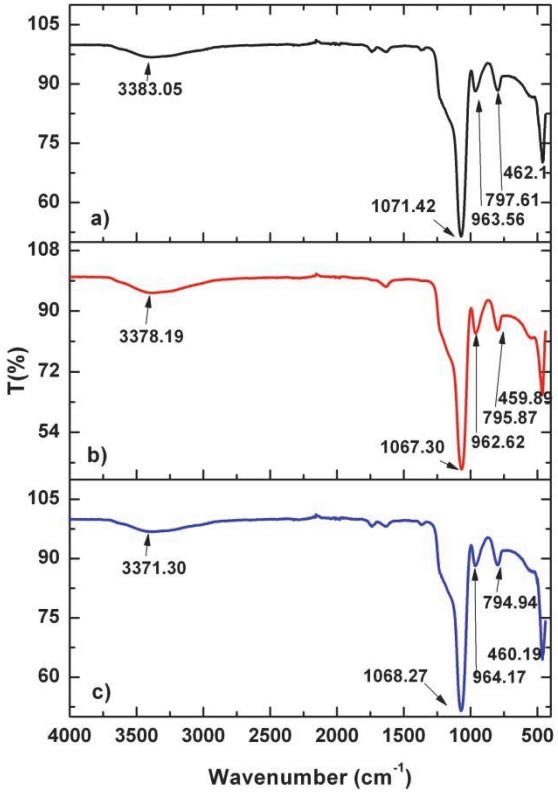

Fig. 3. FTIR spectra of the MCM-48 materials with different templates:
(a) C_{16}TABr, (b) C_{16}TACl, (c) C_{12}TACl

At the equilibrium point, the desorbed amount of U(VI) was in equilibrium with the amount being adsorbed (overall adsorption < 20 mg/g). The same shape of the graphs and the same equilibrium time, suggest that the adsorption process is the same for the tested materials. The elaboration of the materials gives compounds of the same structure but with different characteristics due to the introduction of the different elements. Therefore, a contact time of 5 hours was selected as the optimum parameter for the following experiments.

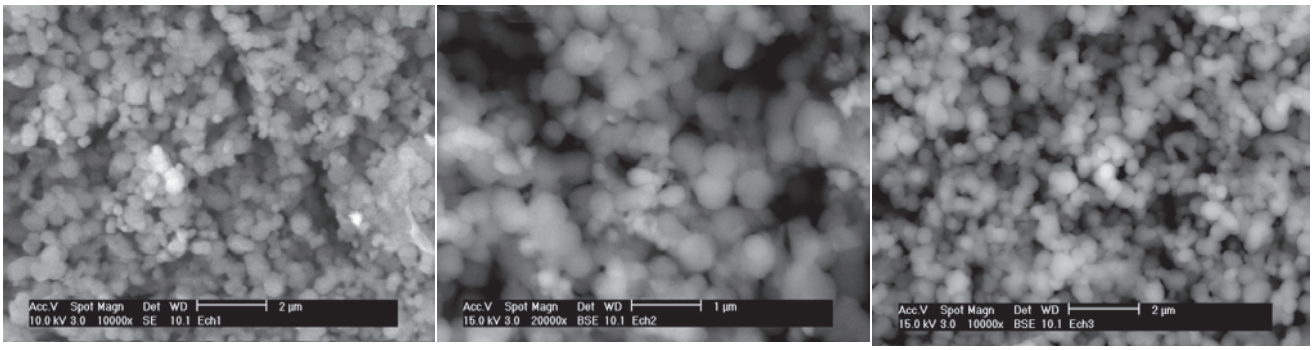

(a) (b) (c)

Fig. 4. Scanning electron micrographs of the MCM-48 materials with different templates: (a) C_{16}TABr, (b) C_{16}TACl, (c) C_{12}TACl

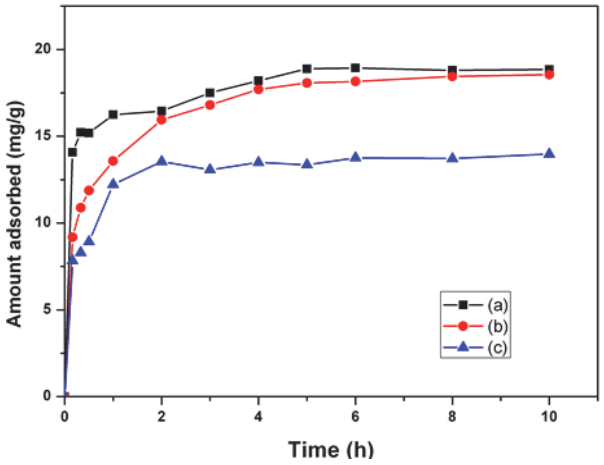

Fig. 5. Effect of contact time on the adsorption of uranium onto the MCM-48 materials with different templates: (a) C_{16}TABr, (b) C_{16}TACl, (c) C_{12}TACl ([U] = 50 mg/L, pH=4, m=21mg, V= 15 mL, T=25°C)

3.2.2. Adsorption mechanism and kinetics

Adsorption is a complex multistep process and kinetic studies will provide valuable insights of the sorption mechanisms which involve mass transfer, diffusion and surface reaction phenomenon. However, the kinetics helps for the prediction of adsorption rate, and the mechanism of the phenomenon which give important information for the modelling the process.

The data of the kinetics of adsorption were analysed using two different kinetic models: the pseudo-first-order and pseudo-second-order models.

- Pseudo-first-order model (Lagergreen, 1889) which has been widely used to predict adsorption kinetics and is given by the following equation (Eq. 3):

$$q = q_e(1 - e^{-K_1 t}) \quad (3)$$

Eq. (3) may be rearranged for linearized data plotting as shown by Eq. (4):

$ln(q_e - q_t) = ln\ qe - k_1 t$, or

$$\log(q_e - q_t) = \log q_e - \frac{k_1}{2.303} t \quad (4)$$

- Pseudo-second-order kinetic model is expressed by Eq. (5) (Plazinski et al., 2013):

$$q_t = \frac{q_e^2 k_2 t}{1 + q_e k_2 t} \quad (5)$$

which can be rewritten as Eq. (6):

$$\frac{t}{q_t} = \frac{1}{k_2 q_e^2} + \frac{t}{q_e} \quad (6)$$

where q_t (mg/g) is the amount of uranium adsorbed on different MCM-48 materials at time t, and q_e (mg/g) is the equilibrium amount adsorbed. The constant k_1 (h^{-1}) and k_2 (g/mg/h) are respectively the adsorption rate constant of pseudo-first and second order kinetic.

The determined parameters from the exploitation of the experimental data are presented in Table 3.

The results show that pseudo-second-order model fits the experimental data quite well, the R^2 values reach the unity and the experimental and theoretical uptakes are in good agreement. This indicates the applicability of the second-order kinetic model to describe the adsorption of uranium (VI) ions by MCM-48 materials. The rate constant for MCM-48 (a) is about 0.28 g/mg/h, as well as the amount adsorbed (≈ 20 mg/g). This was predictable in view of the intrinsic characteristics of the material.

Table 3. Kinetic model parameters

Samples	*Pseudo –first order*			*Pseudo second order*		
	K_1*(1/h)*	q_e*(m/g)*	R^2	k_2*(g/mg/h)*	q_e *(mg/g)*	R^2
MCM-48 (a)	0.28	4.16	0.887	0.28	19.18	0.998
MCM-48 (b)	0.32	9.15	0.894	0.05	19.55	0.996
MCM-48 (c)	0.41	3.74	0.731	0.35	14.16	0.999

3.2.3. Effect of pH

The effect of initial pH of the solution on the maximum uptake capacity of uranium on the different MCM-48 materials was studied using a pH range from 2.0 to 8.0 at 25°C for 5 hours (Fig. 6). It can be seen that the adsorption is strongly dependent on pH value. The amount of uranium adsorbed increases from 0 to 35 mg/g, as pH increases from 2 to 6. The pH of the solution influences the charge of the adsorbent with respect of the point zero charge (Li et al., 2014). This behaviour can be attributed to the synergic effect of functional groups in different MCM-48 materials.

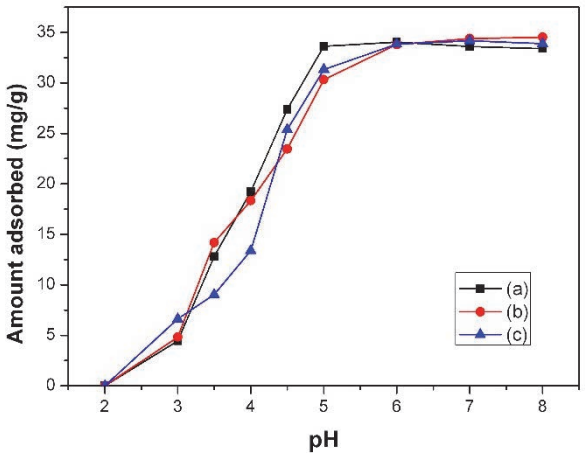

Fig. 6. Effect of pH on the adsorption of uranium onto the MCM-48 materials with different templates: (a) C_{16}TABr, (b) C_{16}TACl, (c) C_{12}TACl ([U] = 50 mg/L, t=5 h, m=21 mg, V= 15 mL, T=25°C)

Otherwise, the pH of point zero charge (pH_{PZC}) for different MCM-48 materials which are found to be approximately 4.6, 4.2 and 3.5 respectively. It is expected that the amount of negative binding sites at different MCM-48 materials can rapidly be increased after pH_{PZC}. On the other hand, the species of uranium are influenced by the pH of the solution; different mononuclear and polynuclear U (VI) hydrolysis products that could be present in aqueous uranium solution as a function of pH (Chen et al., 2013). At pH between 2.0 and 3.0, only UO_2^{2+} is present, from pH 3.0 to 5.0, the polynuclear products $[UO_2(OH)]^+$, $[(UO_2)_2(OH)_2]^{2+}$ and $[(UO_2)_3(OH)_5]^+$ are present with UO_2^{2+}. At pH between 6.0 and 7.0, the hydrolysis is more intense and other polynuclear product $[(UO_2)_4(OH)_7]^+$ and $[(UO_2)_3(OH)_5]^+$ are formed.

As a result, all these species can be adsorbed by the functional groups of different MCM-48 materials. Moreover, at pH higher than 7.0, carbonate uranyl ions $UO_2(CO_3)_2^{2-}$ and $UO_2(CO_3)_3^{4-}$ are formed (Bayou and al., 2017). The next experiments in this study were carried at pH 6.

3.2.4. Adsorption isotherms

Adsorption isotherm provides essential physiochemical data for assessing the applicability of the adsorption process as a complete unit operation. The adsorption of uranium on MCM-48 was carried out under different initial concentrations from 10 to 300 mg/L at pH 6 for 5 hours.

Fig. 7 shows the amount of uranium adsorbed as function of initial uranium concentration.

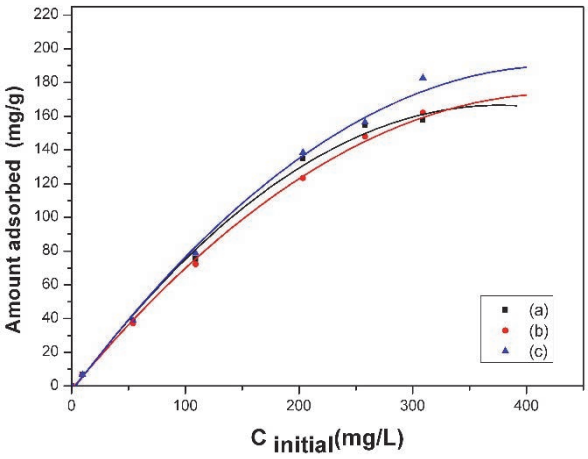

Fig. 7. Effect of initial uranium concentration on the adsorption of U(IV) onto the MCM-48 with different templates: (a) C_{16}TABr, (b) C_{16}TACl, (c) C_{12}TACl (pH = 6, t=5 h, m=21 mg, V= 15 mL, T=25°C)

Langmuir and Freundlich adsorption isotherms models were used to correlate the experimental data. According to the Langmuir model, the saturated monolayer isotherm (Sari et al., 2007) can be Eq. (7):

$$q_e = \frac{q_{max} k_L C_e}{1 + k_L C_e} \tag{7}$$

where q_e (mg/g) is the amount of U(VI) adsorbed per unit mass of adsorbent; C_e (mg/L) is the equilibrium concentration; q_{max} (mg/g) and k_L (L/mg) are Langmuir constants related to adsorption capacity and equilibrium constant related to the affinity of the binding sites and energy of adsorption respectively.

The Freundlich isotherm model assumes that adsorption occurs on a heterogeneous surface through a multilayer adsorption mechanism and that the adsorbed amount is represented by Eq. (8) (Oguz, 2007):

$$q_e = k_F C_e^{1/n} \tag{8}$$

where: k_F ($(mg^{(1-n)}L^n)/g$) is defined as the adsorption capacity of the adsorbent. The *1/n* (dimensionless factor) measures the adsorption intensity or surface heterogeneity.

All constants were calculated according to the slope and the intercept of the related lines. The determined parameters from the exploitation of the experimental data are tabulated in Table 4.

The high values of the correlation coefficients (R^2 >0.98) of Langmuir plot isotherm shows an excellent fit to the experimental data. As noticed, the adsorbed

amounts are consistent (q_{max} >160 mg/g) Moreover, the material MCM48 (a) present an increased affinity (K_L = 0.93 L/g) for the adsorbate.

In comparison to other kinds of adsorbents used under similar experimental conditions (Table 5), the MCM-48 (a) material presents a higher adsorption capacity.

3.2.5. Adsorption thermodynamics

The influence of temperature variation on the adsorption of uranium ions onto MCM-48 was investigated from 25 to 55°C (Fig. 8). From this figure, we can notice that the amount of uranium adsorbed decreases as temperature was increases. This phenomenon, in agreement with the Arrhenius law, suggests that the surface reaction is exothermic and that each temperature increase disadvantages its progress.

Thermodynamic parameters such as standard enthalpy $\Delta H°$ (KJ/mol) and standard entropy $\Delta S°$ (KJ/mol·K), were determined by using Eq. (9) (Kumar and Kacha, 2011):

$$LnK_d = \left(\Delta S^0/R\right) - \left(\Delta H^0/RT\right) \quad (9)$$

where K_d is the distribution coefficient.

The values of enthalpy ($\Delta H°$) and entropy ($\Delta S°$) were obtained by the calculated linear fitting curve of LnK_d as function $1/T$. The standard free energy change was calculated as Eq. (10):

$$\Delta G^0 = -RTLnK_d \quad (10)$$

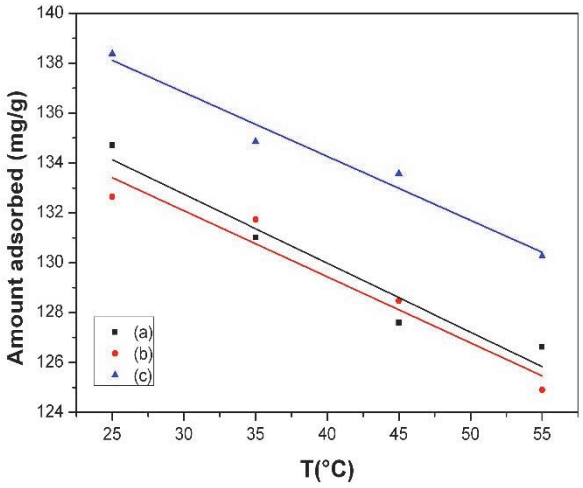

Fig. 8. Effect of temperature on the adsorption of uranium onto MCM-48 with different templates: (a) C_{16}TABr, (b) C_{16}TACl, (c) C_{12}TACl ([U] = 200 mg/L, pH = 6.0, t=5 h, m=21 mg, V= 15 mL)

The values of the thermodynamic parameters for the adsorption of uranium ions on the different MCM-48 are summarized in Table 6.

The observed positive values for the enthalpy suggest that the adsorption of uranium ions is endothermic. Moreover, the negative values of ΔS^0 revealed that the randomness decreased at the different MCM-48 solution interface during the adsorption process. The negative values of ΔG^0 observed for all MCM-48 materials indicate that the adsorption process of uranium is spontaneous and the degree of spontaneity decreases with increasing temperature.

Table 4. Parameters of the isotherm models for uranium adsorption on the MCM-48 materials

Samples	*Langmuir model*			*Freundlich model*		
	q_{max} *(mg/g)*	k_L *(L/g)*	R^2	k_F *((mg$^{(1-n)}$L^n)/g)*	*n*	R^2
MCM-48 (a)	161.29	0.93	0.999	64.31	4.34	0.954
MCM-48 (b)	169.49	0.21	0.978	40.55	3.03	0.974
MCM-48 (c)	185.19	0.49	0.991	65.31	3.71	0.946

Table 5. Comparison of the uranium adsorption capacity of MCM-48 (a) with other adsorbents

Adsorbents	*Experimental conditions*	q_{max} *(mg/g)*	*Reference*
Graphene oxide nanosheets	pH=5, T=20°C	97.5	Zhao et al.(2012)
Carbone nanotubes	pH=6, T= 25°C	137.80	Chen et al.(2018)
Humic acid immobilized Zirconium pillared clay	pH=6, T=30°C	132.68	Anirudhan et al.(2010)
Natural clinoptilolite	pH =6, T=25°C	2.88	Camacho et al. (2010)
MCM-48 (a)	pH=6, T=25°C	161.29	This work

Table 6. Thermodynamic parameters

Samples	*ΔH°* *(KJ/mol)*	*ΔS°* *(J/mol·K)*	*ΔG° (KJ/mol)*			
			298K	*308K*	*318K*	*328K*
MCM-48 (a)	28.87	-56.40	-6.12	-5.43	-4.82	-4.47
MCM-48 (b)	21.43	-52.47	-5.68	-5.32	-5.00	-4.01
MCM-48 (c)	24.20	-57.99	-7.93	-5.67	-5.52	-5.58

4. Conclusions

From the various results obtained in this study, we conclude:

- The mesoporous materials MCM-48 elaborated at room temperature with different templates (C_{16}TABr, C_{16}TACl and C_{12}TACl) as the directing agent of the structure and TEOS as silica source, perfectly fulfilled the role for which they were synthesized. As adsorbent materials, it has a high uranium adsorption capacity greater than 160 mg/g; with an appreciable affinity for the uranium ions of the order of 1 g/L for MCM-48 (a).

- The kinetic studies indicate that the adsorption of uranium ions on MCM-48 can be described by a pseudo-second-order model.

- The adsorption of uranium onto MCM-48 materials was a strongly pH dependent.

- The adsorption equilibrium was fitted by Langmuir equation.

- The value of thermodynamic parameters confirmed the feasibility and spontaneity, as well the endothermic nature of the adsorption process of the uranium ions onto MCM-48 mesoporous materials.

Acknowledgements
We thank Professor Hubert Cabana (University of Sherbrooke, Sherbrooke, Canada) for the corrections made to this work.

References

Anirudhan T., Bringle C.D., Rijith S., (2010), Removal of uranium (VI) from aqueous solutions and nuclear industry effluents using humic acid-immobilized zirconium-pillared clay, *Environmental Radioactivity*, **101**, 267-276.

Bayou N., Ait Amar H., Attou M., Menacer S., (2017), Removal of uranium (VI) from nuclear effluents onto aluminophosphate and silicoaluminophosphate molecular sieves, *Comptes Rendus Chimie*, **20**, 1-6.

Beck J.S., Vartuli J.C., Roth W.J., Leonowicz M.E., Kresge C.T., Schmitt K.D., Chu C.T.U., Olson D.H., Sheppard E.W., McCullen S.B., Higgins J.B., Schlenker J.L., (1992), A new family of mesoporous molecular sieves prepared with liquid crystal template, *American Chemical Society*, **114**, 10834-10854.

Brunauer S., Deming L.S., Deming W.S., Teller E., (1940), On a theory of the van der Waals adsorption of gases, *American Chemical Society*, **62**, 1723-1732.

Camacho L., Deng S., Parra R., (2010), Uranium removal from groundwater by natural clinoptilolite zeolite: Effects of pH and initial feed concentration, *Journal of Hazardous Materials*, **175**, 393-398.

Cerovic L.J.S., Milonjic S.K., Todorovic M.B., Trtanj M.I., Pogozhev Y.S., Blagoveschenskii Y., Levashov E.A., (2007), Point of zero charge of different carbides, *Colloids and Surfaces A: Physicochemical and Engineering Aspects*, **297**, 1-6.

Chellam S., Clifford D.A., (2002), Physical–chemical treatment of groundwater contaminated by leachate from surface disposal of uranium tailings, *Environmental Engineering*, **128**, 942-952.

Chen H., Chen Z., Zhao G., Zhang Z., Xu C., Chen J., Zhuang L., Haya T., Wang X, Liu Y., (2018), Enhanced adsorption of U(VI) and 241 Am(III) from wastewater using Ca/Al layered double hydroxide@carbon nanotube composites, *Journal of Hazardous Materials*, **347**, 67-77.

Chen S.-W., Li Y., Guo B.-L., Song L.-J., Wang Y.-L., (2013), Study on sorption of U(VI) onto ordered mesoporous silicas, *Radioanalytical and Nuclear Chemistry*, **295**, 1435-1442.

Dan H., Ding Y., Lu X., Chi F., Yuan S., (2016), Adsorption of uranium from aqueous solution by mesoporous SBA-15 with various morphologies, *Radioanalytical and Nuclear Chemistry*, **310**, 1107-1114.

Duduman C.N., Los Cobos J.M.G., Harja M., Perrez M.I.B., De castro C.G., Lutic D., Kotovas O., Cretescu I., (2018), Preparation and characterization of nanocomposite material based on TiO_2-Ag for environmental applications, *Environmental Engineering and Management Journal*, **17**, 925-936.

Elabd A., Zidan W.I., Abo-Aly M., Bakier E., Attia M.S., (2014), Uranyl ions adsorption by novel metal hydroxides loaded Amberlite IR120, *Environmental Radioactivity*, **134**, 99-108.

Koyano K.A., Tatsumi T., (1997), Synthesis of titanium-containing MCM-41, *Microprous Materials*, **10**, 259-271.

Kresge C.T., Leonowicz M.E., Roth W.E., Vartuli J.C., Beck J.S., (1992), Ordered mesoporous molecular sieves synthesized by a liquid-crystal template mechanism, *Nature*, **359**, 710-712.

Krestou A., Xenidis A., Panias D., (2003), Mechanism of aqueous uranium (VI) uptake by natural zeolitic tuff, *Minerals Engineering*, **16**, 1363-1370.

Krestou A., Xenidis A., Panias D., (2004), Mechanism of aqueous uranium (VI) uptake by hydroxyapatite, *Minerals Engineering*, **17**, 373-381.

Kumar D., Bera S., Tripathi A.K., Dey G.K., Gupta N.M., (2003), Uranium oxide nanoparticules dispersed inside the mesopores of MCM-48: synthesis and characterization, *Microporous and Mesoporous Materials*, **66**, 157-167.

Kumar D.B., Kacha S., (2011), Study of the kinetics and thermodynamics of the adsorption of a basic dye on sawdust (in French), *Revue des Sciences de L'eau*, **24**, 131-144.

Lagergreen S., (1889), About the theory of so-called adsorption of soluble substances, *Kungliga Svenska Vetenskapsakademiens Handlingar*, **24**, 1-39.

Lee W., Lee Si E., Kim MI-K., Lee Chang H., Kim Young S., (2002), A chelating resin containing 2-(2-thiazolylazo)-5-dimethylaminophenol as the functional group: synthesis and sorption behavior for some trace metal ions, *Bulletin of the Korean Chemical Society*, **23**, 1067-1072.

Li H., Wang X., You W., He D., (2014), Adsorption of Pb (II) from aqueous solution by mesoporous MCM-48, *Dispersion Science* and *Technology*, **36**, 394-401.

Longloiler R., Chaisuwan T., Luengnaruemitchai A., Wongkasemjit S., (2011), Synthesis of MCM-48 from silatrane via sol–gel process, *Sol-Gel Science and Technology*, **58**, 427-435.

Maneesuwan H., Longloilert R., Chaisuwan T., Wongkasemji S., (2013), Synthesis and characterization of Fe-Ce-MCM-48 from silatrane precursor via sol–gel process, *Materials Letters*, **94**, 65-68.

Matei D., Cursaru D.L., Mihai S., (2016), Preparation of MCM-48 mesoporous molecular sieve influence of preparation conditions on the structural properties, *Digest Journal of Nanomaterials* and *Biostructures*, **11**, 271-276.

Melendez-Ortiz H.I., Mercado Y.A., Garcia-Cerda L.A., Merado-Silva J.A., Castruita G., (2014), Influence of the reaction conditions on the thermal stability of mesoporous

MCM-48 silica obtained at room temperature, *Ceramics International*, **40**, 4155-4161.

Mellah A., Chegrouche S., Barkat M., (2006), The removal of uranium (VI) from aqueous solutions onto activated carbon: Kinetic and thermodynamic investigations, *Colloid and Interface Science*, **296**, 434-441.

Miriam B., Debasish D., Rita F., Uwe P., Hermenegildo G., (2006), Urea-containing mesoporous silica for the adsorption of Fe (III) cations, *Chemistry of Materials*, **18**, 5597-5603.

Oguz E., (2007), Equilibrium isotherms and kinetics studies for the sorption of fluoride on light weight concrete materials, *Colloids and Surfaces A: Physicochemical and Engineering Aspects*, **295**, 258-263.

Prasada Rao T., Metild P., Mary Gladis J., (2006), Preconcentration techniques for uranium (VI) and thorium (IV) prior to analytical determination - an overview, *Talanta*, **68**, 1047-1064.

Plazinski W., Dziuba J., Rudzinski W., (2013), Modeling of sorption kinetics: the pseudo-second order equation and the sorbate intraparticle diffusivity, *Adsorption*, **19**, 1055-1064.

Reza D., Rojaee A., Heshmatipour Z., (2018), Thermodynamics, kinetics and equilibrium studies of uranium sorption by Gracilaria corticata red alga, *Environmental Engineering and Management Journal*, **17**, 1199-1208.

Sari A., Tuzen M., Citak D., Soylak M., (2007), Equilibrium, kinetic and thermodynamic studies of adsorption of Pb (II) from aqueous solution onto Turkish kaolinite clay, *Hazardous Materials*, **149**, 283-291.

Selvam P., Bhatia S.K., Sonwane C., (2001), Recent advances in processing and characterization of periodic mesoporous MCM-41 silicate molecular sieves, *Industrial & Engineering Chemistry Research*, **40**, 3237-3261.

Schmidt R., Stocker M., Akporiaye D., Heggelund Torstad M., Olsen A., (1995), High-resolution electron microscopy and X-ray diffraction studies of MCM-48, *Microporous Materials*, **5**, 1-7.

Shen Y., Tan X., Wang L., Wu W., (2011), Extraction of the uranyl ion from the aqueous phase into an ionic liquid by diglycolamide, *Separation and Purification Technology*, **78**, 298-302.

Tavakoli H., Sepehrian H., Cheraghali R., (2013), Encapsulation of nanoporous MCM-41 in biopolymeric matrix of calcium alginate and it use as effective adsorbent for lead ions: Equilibrium, kinetic and thermodynamic studies, *Taiwan Institute of Chemical Engineers*, **44**, 343-348.

Wang L., Zhang J., Chen F., (2009), Synthesis of hydrothermally stable MCM-48 mesoporous molecular sieve at low cost of CTAB surfactant, *Microporous and Mesoporous Materials*, **122**, 229-233.

Zhang J.-Y., Zhang N., Zhang L., Fang Y., Deng W., Li L., Liu X., Li I., Yu M., (2015), Adsorption of Uranyl ions on amine functionalization of MIL101 (Cr) nanoparticles by a facile coordination based Post-synthetic strategy and X-ray absorption spectroscopy studies, *Scientific Reports*, **5**, 13514-13524.

Zhao G., Wen T., Yang X., Yang S., Liao J., Hu J., Shao D., Wang X., (2012), Preconcentration of U(VI) ions on few-layered graphene oxide nanosheets from aqueous solutions, *Dalton Transactions*, **41**, 6182-6188.

Zuo L., Shaming Y., Hai Z., Xue T., Jun J., (2011), Th (IV) adsorption on mesoporous molecular sieves: effects of contact time, solid content, pH, ionic strength, foreign ions and temperature, *Radioanalytical and Nuclear Chemistry*, **288**, 379-387.